Journal of Experimental and Applied Physics
Journal Homepage: jeap.ppj.unp.ac.id
Vol. 1, No. 3, December 2023.
ISSN (Print): 2988-0378 ISSN (Online): 2987-9256

Analysis of Earthquake Fault Types 2022 in The Mentawai Region using Waveform Inversion Method

Ika Sri Fahmi[1], Syafriani[1,*], Hamdi[2], Letmi Dwiridal[3]

[1] *Department of Physics, Universitas Negeri Padang, Padang 25131, Indonesia*
[2] *Department, University/Institution, City ZIP Code, Country*

Article History
Received : December, 26th 2023
Revised : December, 30th 2023
Accepted : December, 31th 2023
Published : December, 31th 2023

DOI:
https://doi.org/10.24036/jeap.v1i3.34

Corresponding Author
*Author Name: Syafriani
Email: syafri@fmipa.unp.ac.id

Abstract: Indonesia is a country prone to earthquake disasters, because Indonesia is located in the collision area between plates, and one of the areas in Indonesia where plate movements often occur is Mentawai. Analysis of waveform data on the 2022 earthquake in the Mentawai region was carried out to determine the type of fault. The data used in this research is local seismic data downloaded from webdc.eu. Seismic data was analyzed using waveform inversion method implemented in ISOLA program. In the ISOLA program, data processing is carried out which includes: inputting 3-component seismic data, earthquake info events, selecting stations, green functions, performing inversion, and displaying results in the form of tensor moment values, strike, dip, and rake values. From the data analysis, the moment tensor value is obtained with the range of each component of M11 is -8.348 to -3.673, M22 is 0.710 to -2.037, M33 is 7.639 to 5.710, M31 is 2.050 to 3.761, M32 is 3.484 to -5.672, M12 is -2.751 to 2.455. Then the inversion results obtained in the form of fault parameters, namely strike, dip, and rake for two nodals that will be analyzed to determine the fault plane. Based on the moment tensor value, it is found that the type of earthquake fault in 2022 in Mentawai region is dominated by reverse fault and oblique fault patterns.

Keywords: Waveform inversion, ISOLA, Moment Tensors, Strikes, dip, Rake

1. Introduction

A fault is a gap in the Earth's crust at the boundary between two tectonic plates [1]. The deformed earth's crust will accumulate energy. This deformed energy will continue to accumulate until one day it causes vibrations on old faults or creates new faults in the earth's crust. Faults found on the surface of bedrock are weak planes where earthquake sources occur. Indonesia is known as an area prone to natural disasters, one of which is earthquakes. This is because Indonesia is located at the meeting point of three major plates in the world, namely the Indo-

How to cite:
I. S. Fahmi, Syafriani, Hamdi, L. Dwiridal, 2023, Analysis of Earthquake Fault Types 2022 in The Mentawai Region using Waveform Inversion Method, *Journal of Experimental and Applied Physics,* Vol.1, No.3, page 62-72. https://doi.org/10.24036/jeap.v1i3.34

Australian Plate in the South, the Eurasian Plate in the West and the Pacific Ocean Plate in the East [2]. The movement of these plates causes friction, pressure and pressure on the areas where they meet . The pressure arising from the movement of the plates continues to grow. So, at some point when it cannot withstand the great pressure, the rock becomes broken and lifted. The release of this pressure causes vibrations or waves. The waves then spread in all directions from the point where the rock breaks or lifts and produce shocks/vibrations on the earth called earthquakes [3].

One of the areas in Indonesia that often experience earthquakes is the Mentawai region which is geographically located at latitudes 0° 55' 00" LU - 30° 21' 00" LU and 98° 35' 00" East - 100° 32' 00" East with an area of about 6,011.35 km2. Mentawai has about 4 big islands and 252 small islands with a total population of 68,807 people. The seismicity in Mentawai is very high due to the meeting of two plates, namely the Indo-Australian Ocean Plate which moves from the southwest and subducts into the Eurasian Continental Plate located in the northeast [4]. The Indo-Australian Ocean Plate that continuously subducts under the Eurasian Continental Plate results in the formation of a subduction zone. This subduction zone activity can cause shallow and medium earthquakes in Mentawai. If the depth of the earthquake is shallow and the fault is a rising fault, it has the potential to cause a tsunami [5].

Due to the activity of the subduction zone and active faults, the Mentawai region has quite a significant earthquake record. This can be seen from the occurrence of previous earthquakes with epicenters on land and shallow depths, which are thought to be due to local fault activity that has caused considerable casualties and infrastructure damage, so that the same threat in areas indicated to have active fault structures will always lurk[6] . To reduce the damage caused by earthquakes, it is necessary to know the types of earthquake faults [7] . Understanding the types of faults that cause earth quakes is necessary to understand the character and consequences of earthquakes [8].

The method that can be used to determine the type of earthquake fault is the wave inversion method. This method utilizes the P-wave arrival time and is estimated using a three-component Green's function [9]. The inversion method using waveforms has advantages when compared to using travel time data, because in this method the origin and depth of the centeroid are closely related to each other [10] . A good inversion process is based on the matching of observation data and synthetic data from the inversion. Good results occur when the observation data and synthetic data overlap.

The wave inversion method is implemented in the ISOLA software [11]. ISOLA is a Fortran software for calculating moment tensors that is executed by using the Matlab . ISOLA program processing uses instrument correction to the seismogram used, provides tools to filter data that can eliminate noise, so that the results obtained will be better [12]. Based on these problems, a research was conducted to analyze the type of faults in the Mentawai region using the wave inversion method. From the results of the fault type analysis, it is expected to be able to predict the tectonic state and can be known areas that have the potential for large earthquakes, so that later it can be used as a reference for mitigating earthquake disasters that occur in the disaster area.

2. Materials and Method

The data used in this research is the data of earthquake events in Mentawai region in 2022 with magnitude ≥ 5 SR. This earthquake data can be downloaded through WebDC which can be

accessed through iris.edu. This research uses wave inversion method. The earthquake data were processed in ISOLA software developed to obtain the earthquake source parameters. The earthquake source parameters are estimated from the inversion model using Green's function [13]. Mathematically, Green's function can be seen in equation 1:

$$U_k\ (\mathrm{r,t}) = \sum_{i=6}^{6} G_{ki\ (r,c,t)} * f_i\ (\mathrm{c,t}) \qquad (1)$$

Where Uk is the displacement recorded in the kth component, r is the receiver position, c is the position of the earthquake source (centroid). Gki is the Green's function, depending on the elastic and anelastic properties of the earth. The asterisk indicates convolution, fi(c, t) represents the six independent components of the moment tensor. Green's function can be used for the moment tensor of earthquake event data. The moment tensor concept can provide a complete picture of the forces from a seismic point source . In general, the moment tensor [Mjk] has 6 independent basic moment tensor components. If Gki (r, c, t) is a Green's function that also represents the synthetic seismogram at the kth station and the jth principal tensor; Mjk. The observed seismogram is denoted by Uk(r,t), then the estimated ai coefficients for Mjk can be found. The equation for the moment tensor component Mjk in spherical coordinates can be seen in equation 2:

$$\mathrm{M_{jk}} = \begin{bmatrix} M_{11} & M_{12} & M_{13} \\ M_{21} & M_{22} & M_{23} \\ M_{31} & M_{32} & M_{33} \end{bmatrix} \begin{bmatrix} M_{xx} & M_{xy} & M_{xz} \\ M_{xy} & M_{yy} & M_{yz} \\ M_{xz} & M_{yz} & M_{zz} \end{bmatrix} \qquad (2)$$

Where Mjk is the moment tensor component in direction k with normal plane jk . The right-hand column vector is a composite of the observed seismogram results and the left-hand column vector is a composite of the synthetic displacement of a source unit calculated with the six basic elements of the moment tensor [14]. These moment tensor components are used to describe the direction of the force that causes an earthquake to occur [6]. The force traveling in direction j with respect to k is denoted in Mjk, which is a component of the moment tensor. The nine components of the moment tensor are expressed in Figure 1 as follows:

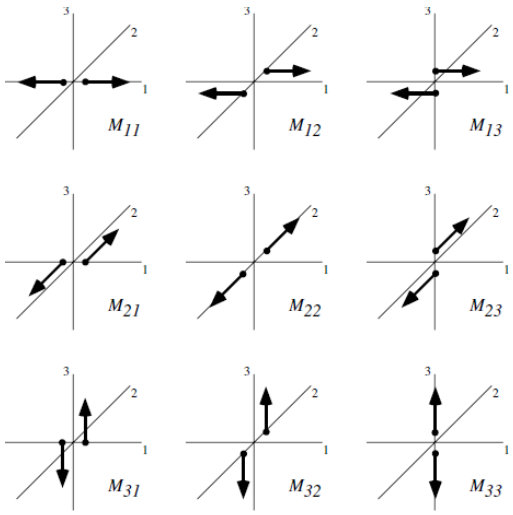

Figure 1. Force Pairs of Moment Component tensors (Shearer, 2009) [15]

The force moving in direction j with respect to k is symbolized in Mjk which is the moment tensor component. The nature of this moment tensor is symmetrical, because Mjk is equal to Mkj. The value of the Mijk component can be used to determine the strike (φ), dip (δ) and rake (λ) parameters that cause earthquakes. Because Mjk = Mkj, there are only 6 independent moment tensors [16]. The relationship between moment tensor and strike (φ), dip (δ) and rake (λ) is expressed in equation 3 :

$$
\begin{aligned}
Mxx &= -Mo\,(\sin\delta.\cos\lambda.\sin 2\phi + \sin 2\delta.\cos\lambda.\sin^2\phi)\\
Mxy &= Myx = Mo\,(\sin\delta.\cos\lambda.\sin 2\phi + \tfrac{1}{2}.\sin 2\delta.\cos\lambda.\sin 2\phi)\\
Mxz &= Mzx = -Mo\,(\cos\delta.\cos\lambda.\cos\phi + \cos 2\delta.\sin\lambda,\sin 2\phi)\\
Myy &= Mo\,(\sin\delta.\cos\lambda.\sin 2\phi - \sin 2\delta.\sin\lambda.\cos 2\phi)\\
Myz &= Mzy = -Mo\,(\cos\delta.\cos\lambda.\sin\phi - \cos 2\delta.\sin\lambda.\cos\phi)\\
Mzz &= Mo\,(\sin 2\delta.\sin\lambda)
\end{aligned}
\qquad (3)
$$

The value of these components is used to determine the strike (ϕ), dip (δ), and rake (λ) parameters that cause earthquakes. Strike is the angle formed by the fault plane with the north direction. Dip is the angle formed by the fault plane with the horizontal plane and measured in the vertical plane with its direction perpendicular to the fault line. Rake is the angle formed by the slip direction and the fault line. Earthquake parameters can be known from the results of earthquake data analysis, namely seismic waves. The data used to determine the characteristics of earthquakes is waveform data or three-component local waveform [17]. Furthermore, the waveform data inversion process and determining the magnitude of the moment tensor were carried out using ISOLA software . In the first step, data from IRIS Wilber 3 in the form of earthquake data in SAC format. Then input the earthquake data in SAC import. After that, the definition of earthquake event info is to enter the value of earthquake parameters such as latitude, longitude, and depth. Then enter the value of the crustal model, followed by the selection of the earthquake station that will be used for tensor moment processing [18]. After all the data used is inputted, then prepare the data to be used before further processing is carried out. Processing involving seismograms consists of performing instrument correction, origin time alignment and resampling, filtering by selecting low and high frequencies to minimize noise, and preparing data for the inversion process. In the next stage, seismic source definition is performed by determining the initial depth, depth range, and number of seismic sources that will be used for the inversion process.

After all the data preparation is complete, the Green's function calculation is performed. Green's function serves to calculate a synthetic seismogram that will be matched with seismogran data to estimate suitable parameters in the inversion process and then the inversion process involves three seismogram components by selecting the right filter. This aims to remove noise before performing the inversion process. From the processing using ISOLA, the moment tensor solution and the focal mechanism of the earthquake are displayed in the form of a beach ball so as to be able to know the fault pattern that causes the earthquake, the parameters of the earthquake source, and the direction of the force that causes the earthquake [19]. The diagram of the beach ball can be seen in Figure 2:

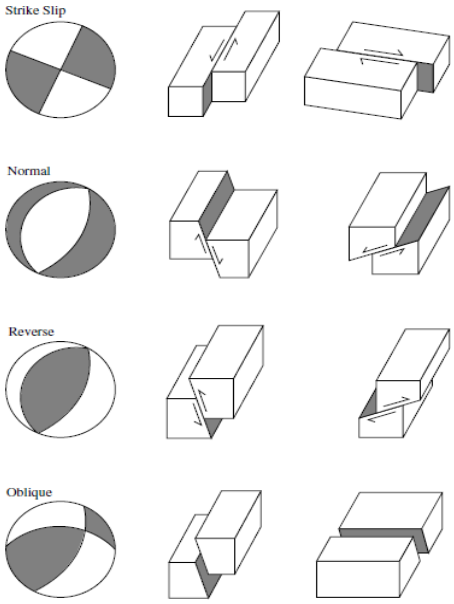

Figure 2. Focal mechanism pattern (beachball)

Based on figure 2, strike-slip faults, the fault movement is horizontal. Normal faulting occurs when the hanging wall descends relative to the foot wall, the fault plane has a large dip, usually called a down fault. Then a reverse fault occurs when the hanging wall rises relative to the foot wall, the fault plane has a large slope, usually called a rising fault . Oblique faults are fault movements that are a combination of vertical and horizontal. The forces at work cause strike-slip faults and normal faults [20] . The beach ball pattern formed will produce two colors, namely black and white in the same beachball. Where for the white color will suppress the black area. So it can be concluded that the black color will experience strong pressure and the white color will experience strain.

3. Results and Discussion

The data used is earthquake data in 2022 in Mentawai region with magnitude ≥ 5SR. In this earthquake data, there are eight stations selected, namely the eight closest stations. The eight selected stations can be seen in Figure 3:

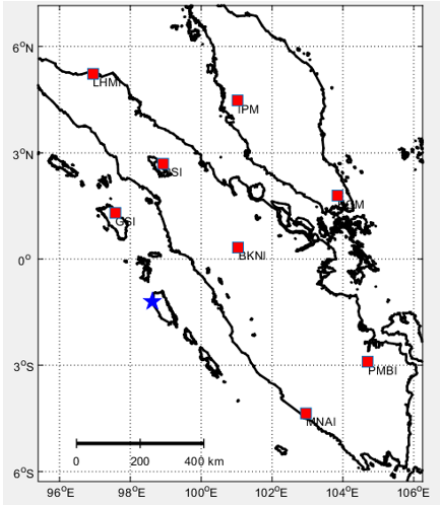

Figure 3. Stations used in the study.

The stations used in the study are GSI, BKNI, PSI, MNAI, KOM, IPM, PMBI, and LHMI. This station contains network geographic coordinate information useful for selecting stations to be used in inversion . This research was processed using waveform inversion method. This data processing uses the green function equation found in equation 1. From the results of the green function, the value of the tensor moment is obtained. The calculation of the tensor moment value using the ISOLA program, so that the tensor moment value can be seen in table 1 below:

Table 1. Moment Tensor for the 2022 Mentawai earthquake event.

Event	M_{rr} = M33	M_{tt} = M11	M_{pp} = M22	M_{rt} = M31	M_{rp} = M32	M_{tp} = M12
2022-06-24_18:56:33	7.639	-8.348	0.710	2.050	3.484	-2.751
2022-08-28_22:34:36	4.550	-4.332	-0.218	-4.162	0.069	1.035
2022-08-29_03:29:13	-0.241	-0.174	0.416	5.448	-6.496	0.154
2022-09-10_23:10:43	1.634	-1.045	-0.590	1.507	-1.935	0.841
2022-09-10_23:24:00	7.982	-2.696	-5.286	0.600	-0113	0.754
2022-09-20_22:25:01	5.710	-3.673	-2.037	3.761	-5.672	2.455

Based on table 1, it can be seen that Mrr range from -0.241 to 7.982, Mtt range from -8.348 to -0.174, Mpp range from -5.286 to 0.710, Mrt range from -4.162 to 5.448, Mrp range from -6.496 to 3.484, Mtp range from -2.751 to 2.455. From the value of the moment tensor, the value of the two fault planes, namely the fault plane and auxiliary plane contained in equation 2. The value of the two fault planes can be seen in table 2:

Table 2. Fault plane and auxiliary plane for the 2022 Mentawai earthquake events

Event	PlaneI			PlaneII		
	Strike	Dip	Rake	Strike	Dip	Rake
2022-06-24_18:56:33	56	58	67	274	39	122
2022-08-28_22:34:36	111	25	105	275	66	83
2022-08-29_03:29:13	320	90	-92	230	3	0
2022-09-10_23:10:43	139	73	97	296	18	67
2022-09-10_23:24:00	162	46	86	348	44	94
2022-09-20_22:25:01	141	71	100	294	21	65

Table 2 is the value of fault plane and auxiliary plane for the 2022 Mentawai earthquake events. Where the value of plane 1 the highest strike value is 320, the highest dip value is 90, and the highest rake value is 100. While the value of plane 2 the highest strike value is 348, the highest dip value is 66, and the highest rake value is 122. Based on the analysis of the values of table 1 and table 2, data processing is carried out using ISOLA software, so that the parameter values of each earthquake event can be seen in Table 3:

Table 3. Parameters of each 2022 Mentawai earthquake event.

Event	CD (Km)	VR (%)	DC (%)	CN (%)	STVAR (%)	FMVAR (%)
2022-06-24_18:56:33	9	0.53	89.6	4.6	0.01	57
2022-08-28_22:34:36	13	0.51	97.8	3.4	0.14	44
2022-08-29_03:29:13	3	0.64	94.9	9.4	0.05	7
2022-09-10_23:10:43	10	0.73	98.5	2.9	0.21	51
2022-09-10_23:24:00	11	0.76	37.1	8.7	0.07	28
2022-09-20_22:25:01	12	0.8	85.6	2.5	0.09	10

Based on table 3, the percentage value of reduction variation (VR) > 5% is obtained, namely from 0.51% to 0.8%. This VR value is declared accurate. The double couple (DC) value obtained is from 37.1% to 98.5%, so it can be defined that the earthquake occurred from tectonic activity because the DC value is > 50%. Then the percentage value of the tensor moment resolution (CN) shows an accurate value because the value obtained in the processing is <10%, namely 2.5% to 9.4%. As for the STVAR and FMVAR values that show the value obtained from the results of data processing <30% and the STVAR value >0.30%, so it can be concluded that the results of the solution of the focal mechanism between the position of the earthquake and the time of the centeroid are correct or accurate. The parameter values of each earthquake event can also be seen in one of the tensor moment results for the earthquake event on 29-08-2022_03:29:13. The following tensor moment results are found in Figure 4:

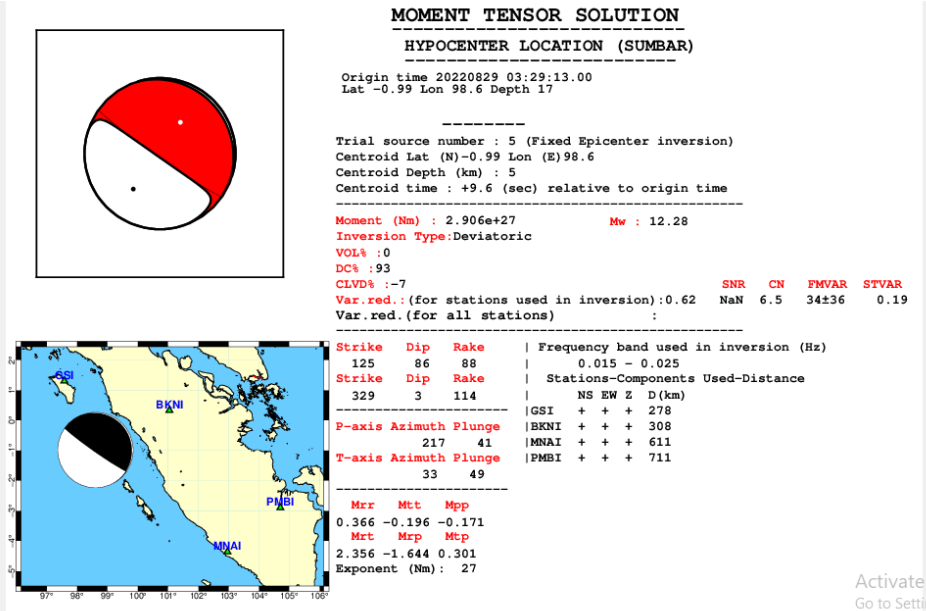

Figure 4. Moment tensor results

Figure 4 is the result of the moment tensor obtained in the research using ISOLA software. In the moment tensor solution there are tensor moment values, beach ball patterns, strike, dip, rake values, and earthquake event parameter values listed in tables 1, 2, and 3. These earthquake source parameters are estimated using an inversion model to achieve good three-component waveform fitting. A good inversion process is based on the matching results of observation data

and synthetic data from the inversion, where good results occur when the observation data and synthetic data overlap. Comparison of the results of observation data and synthetic data as show in figure 5 below:

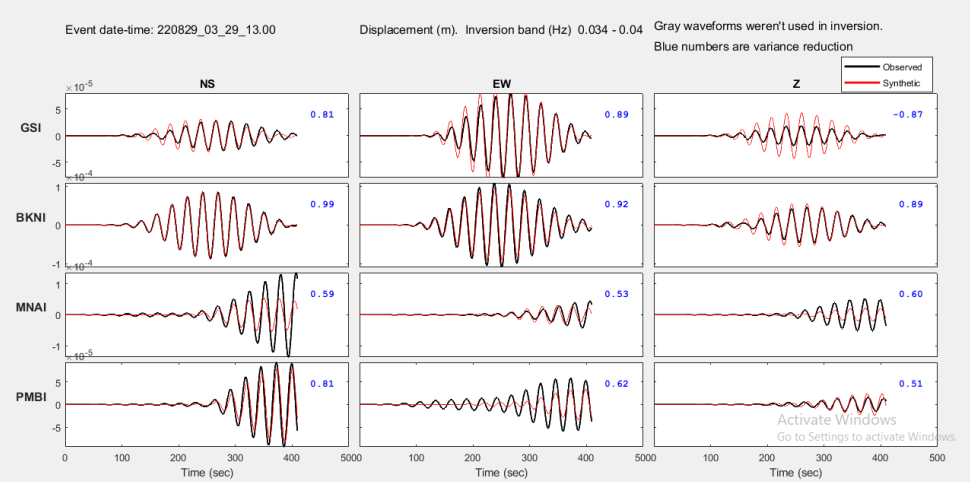

Figure 5. Fitting kurva observed and synthetic waveforms.

In Figure 5, the observed and synthetic waveforms overlap, which shows that the results are quite accurate because they are in the >0.5 range. This correlation is fairly good when viewed from curve fitting. The correlation between observations and synthetics gets better as it approaches 1. This means that the observational and synthetic data have a good match. Then the results of the moment tensor are analyzed to determine the direction of the force that caused the earthquake, so that the type of fault can be known, which is described by the beach ball pattern in Figure 6.

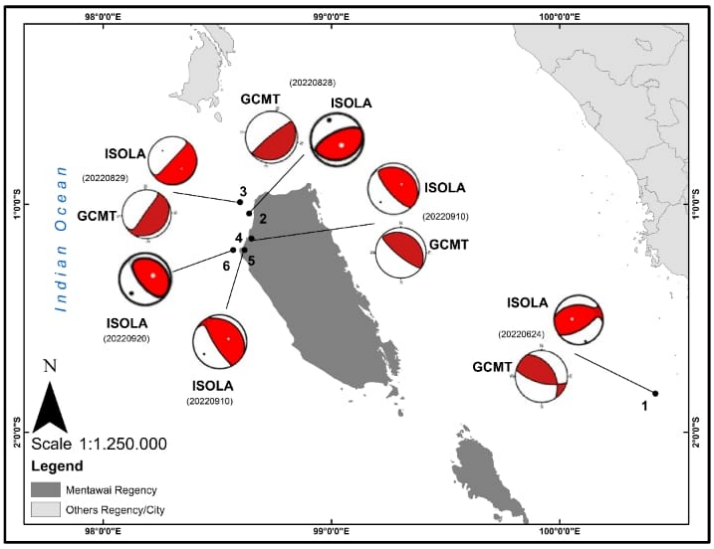

Figure 6. The position of the beach ball depicting the epicenter position

In Figure 6, we can see the comparison between the data processed in the ISOLA program and the results of the processing and depiction of beach balls in the GCMT program for each earthquake event. There are results of the type of faults that occur in local earthquake events in

the Mentawai region are ascending faults and horizontal faults. The reverse fault pattern is found in the beach ball of earthquake events 2, 3, 4, 5, and 6, while the oblique fault pattern is found in the beach ball of earthquake event 1. In the comparison of beach ball pattern 5, there is no GCMT beach ball pattern, this is because the earthquake event on that date was an aftershock. The processing results using ISOLA and GCMT results do not have too much difference, so it can be said that the processing results in this study are quite accurate.

Earthquake source parameters for the Mentawai region in 2022 have been generated and reported by several institutions, one of which is GCMT. The results of this study can be used as a comparison. Researchers used GCMT as a comparison because it has different methods from the ISOLA method. GCMT uses tele-seismic data and uses a global velocity model whose wave equation solution uses spherical coordinate equations, while ISOLA software uses local earthquake data and uses a local velocity model whose equation solution uses cartesian coordinate equations.

It can be seen in the distribution map above, a comparison between the ISOLA and GCMT beach ball shapes at each earthquake event. ISOLA has a beachball shape that is quite similar to the beach ball shape given by GCMT. This means that determining the type of earthquake fault and moment tensor using the waveform inversion method can be applied. Based on this study, the depiction of the beach ball position in Figure 6 shows that the fault planes formed in the Mentawai region are dominated by reverse faults and oblique faults. This condition is influenced by the regional geology of Mentawai.

4. Conclusion

Based on the research that has been done, it can be concluded that the results of the tensor moment obtained in the 2022 earthquake event in the Mentawai region are M11 is -8.348 to 0.615, M22 is 0.710 to 0.422, M33 is 7.639 to -1.037, M31 is 2.050 to -0.798, M32 is 3.484 to 1.825, M12 is -2.751 to -0.099. From the results of the moment tensor, it is found that the type of earthquake faults that occur in the Mentawai region are reverse faults and oblique faults.

Acknowledgments

The authors would like to thank WebDC 3 and GCMT as data sources in this research, as well as Sokos and Zahradnik for the ISOLA program along with its instructions and tutorials that have facilitated the research process, and others who have helped this research.

References

[1] M. Greene, M. Power, and L. T. Youd, "Earthquake Basics," *Earthquake*, no. Figure 4, p. 8, 1994.

[2] G. Pasau and A. Tanauma, "Pemodelan Sumber Gempa Di Wilayah Sulawesi Utara Earthquake Source Modeling of North Sulawesi Region As," *J. Ilm. Sains*, vol. 11, no. 2, pp. 203-209D, 2011.

[3] I. Setyowidodo and B. J. Santoso, "Terhadap Moment Tensor Gempa Bumi Di," vol. 3, no. 2, pp. 113–128, 2011.

[4] M. Sumber and G. Bumi, "928X Print) 86," vol. 3, no. 2, 2014, [Online]. Available: www.ngdc.noaa.gov.

[5] R. G. Gordon, C. DeMets, and J. Y. Royer, "Evidence for long-term diffuse deformation of the lithosphere of the equatorial Indian Ocean," *Nature*, vol. 395, no. 6700, pp. 370–374, 1998, doi: 10.1038/26463.

[6] F. Hilmi and I. Haryanto, "Pola Struktur Regional," *Bull. Sci. Contrib.*, vol. 6, no. 1, pp. 57–66, 2008.

[7] R. McCaffrey, "The tectonic framework of the sumatran subduction zone," *Annu. Rev. Earth Planet. Sci.*, vol. 37, pp. 345–366, 2009, doi: 10.1146/annurev.earth.031208.100212.

[8] S. Continental, "Se i smotecton i cs of Pen i nsular Ind i a and Sr i Lanka," no. 1989, 2003.

[9] E. N. Sokos and J. Zahradnik, "ISOLA a Fortran code and a Matlab GUI to perform multiple-point source inversion of seismic data," *Comput. Geosci.*, vol. 34, no. 8, pp. 967–977, 2008, doi: 10.1016/j.cageo.2007.07.005.

[10] N. Sciences and U. N. Surabaya, "Determining the Source Parameters of the Jambi Earthquake (1 October 2009 , M w = 6 . 4) Using Three-Component Local Waveforms," vol. 1, no. October 2009, pp. 17–22, 2013.

[11] E. Sokos and J. Zahradník, "Evaluating centroid-moment-tensor uncertainty in the new version of ISOLA software," *Seismol. Res. Lett.*, vol. 84, no. 4, pp. 656–665, 2013, doi: 10.1785/0220130002.

[12] J. Zahradník and E. Sokos, "The Mw 7.1 van, eastern turkey, earthquake 2011: Two-point source modelling by iterative deconvolution and non-negative least squares," *Geophys. J. Int.*, vol. 196, no. 1, pp. 522–538, 2013, doi: 10.1093/gji/ggt386.

[13] J. Zahradník, A. Serpetsidaki, E. Sokos, and G. A. Tselentis, "Iterative deconvolution of regional waveforms and a double-event interpretation of the 2003 Lefkada earthquake, Greece," *Bull. Seismol. Soc. Am.*, vol. 95, no. 1, pp. 159–172, 2005, doi: 10.1785/0120040035.

[14] H. Kanamori, L. Rivera, and W. H. K. Lee, "Historical seismograms for unravelling a mysterious earthquake: The 1907 Sumatra Earthquake," *Geophys. J. Int.*, vol. 183, no. 1, pp. 358–374, 2010, doi: 10.1111/j.1365-246X.2010.04731.x.

[15] M. Båth, "Introduction to Seismology," *Geophys. J. R. Astron. Soc.*, vol. 40, no. 1, pp. 143–143, 1975, doi: 10.1111/j.1365-246X.1975.tb01612.x.

[16] J. Schweitzer and T. Lay, "IASPEI: Its origins and the promotion of global seismology," *Hist. Geo. Space Sci.*, vol. 10, no. 1, pp. 173–180, 2019, doi: 10.5194/hgss-10-173-2019.

[17] C. P. Fahntalia and Madlazim, "Pengaruh Jumlah Stasiun Seismik Terhadap Hasil Estimasi Centroid Moment Tensor Gempa Bumi," *J. Inov. Fis. Indones.*, vol. 06, no. 03, pp. 1–5, 2017, [Online]. Available: http://202.90.198.100/webdc3/,

[18] M. Madlazim, "Estimasi Durasi, Arah Dan Panjang Rupture Serta Lokasi-Lokasi Gempa Susulan Menggunakan Perhitungan Cepat," *J. Penelit. Fis. dan Apl.*, vol. 1, no. 2, p. 8, 2011, doi: 10.26740/jpfa.v1n2.p8-18.

[19] E. Djauhari, "Membangun Fungsi Green dari Persamaan Difrensial Linear Non Homogen Tingkat - n," *J. Mat. Integr.*, vol. 11, no. 2, p. 119, 2016, doi: 10.24198/jmi.v11i2.9423.

[20] M. I. Alim, A. H. Safrian, D. Sungkono, and P. B. J. Santosa, "Estimasi Pola Bidang Sesar dan Momen Tensor Gempa Kawasan Laut Selatan bagian Jawa Barat," *J. Dep. Fis. Fak. Ilmu Alam Inst. Teknol. Sepuluh Nop.*, no. January, 2018, doi: 10.13140/RG.2.2.12161.10086.